An Energy Management System for Joint Operation of Small-Scale Wind Turbines and Electric Thermal Storage in Isolated Microgrids

Jinshun Su*, Payman Dehghanian†, Benedict Vergara‡
Department of Electrical and Computer Engineering
The George Washington University
Washington, DC, USA.
{*jsu66, †payman, ‡benvergara96}@gwu.edu

Mohammad Heidari Kapourchali
Department of Electrical Engineering
University of Alaska Anchorage
Anchorage, AK, USA.
mhkapourchali@alaska.edu

2021 North American Power Symposium (NAPS) | 978-1-6654-2081-5/21/$31.00 ©2021 IEEE | DOI: 10.1109/NAPS52732.2021.9654467

***Abstract*—Unlike stationary wind turbines, a small-scale mobile wind turbine (MWT) can travel, via a truck, between isolated microgrids (MGs) to meet the supply-demand balance requirements locally. This spatio-temporal flexibility can bring benefits to the system operators and the energy management system (EMS) performance across MGs. Another flexible resource, electric thermal storage (ETS), can also unlock capabilities for the EMS by maximizing the renewable energy utilization and shifting demand. This paper develops an EMS optimization model for joint operation of MWT and ETS in isolated MGs. The proposed model is formulated as a mixed-integer linear programming (MILP) problem. Case studies of an integrated transportation and energy network — a Sioux Falls transportation network and four IEEE 33-node distribution systems — demonstrate the operating cost reduction and highlight the load shifting benefits of jointly operating MWT and ETS.**

***Index Terms*—Energy management system (EMS), mobile wind turbine (MWT), electric thermal storage (ETS), mixed-integer linear programming (MILP), load shifting.**

NOMENCLATURE

A. Indices and Sets

$\phi \in \mathbf{\Phi}$	Index and set of microgrids (MGs).
$i, j \in \mathbf{B}$	Index and set of nodes in MGs.
$\psi \in \mathbf{\Psi}$	Index and set of upstream systems.
$t, \tau \in \mathbf{T}$	Indices and set of time periods.
$l(i,j) \in \mathbf{L}$	Index and set of branches in the MGs.
$g \in \mathbf{G}$	Index and set of diesel generators (DGs).
$w \in \mathbf{W}$	Index and set of mobile wind turbines (MWTs).
$e \in \mathbf{E}$	Index and set of energy storage systems (ESSs).
$v \in \mathbf{V}$	Index and set of Photovoltaics (PV).
$m, n \in \mathbf{N}$	Indices and set of nodes in the transportation system (TS).
$\mathbf{N^d} \in \mathbf{N}$	Subset of nodes that are depots in the TS.
$\mathbf{\Psi}_i \in \mathbf{\Psi}$	Subset of upstream systems that are connected to node i.
$\mathbf{G}_i \in \mathbf{G}$	Subset of DGs that are connected to node i.
$\mathbf{E}_i \in \mathbf{E}$	Subset of ESSs that are connected to node i.
$\mathbf{V}_i \in \mathbf{V}$	Subset of PVs that are connected to node i.
$\mathbf{W}_i \in \mathbf{W}$	Subset of MWTs that are connected to node i.

B. Parameters and Constants

$c^{up}_{\psi,t}$	Price for buying power from upstream network ψ at time t [$/kW].
a_g	Power generation cost of DG unit g [$/kW].
b_g, c^{su}_g, c^{sd}_g	No-load/start-up/shut-down costs of DG g [$].
c^{ets}	Self-discharge cost of electric thermal storage (ETS) [$/kW].
$\mu_{\phi,t}$	Percentage of electric heating demand replaced by (ETS) in MG ϕ at time t.
$\delta_{\phi,t}$	Percentage of electric demand for heating in MG ϕ at time t.
$P^d_{i,\phi,t}, Q^d_{i,\phi,t}$	Forecasted real/reactive demand of node i in MG ϕ at time t [kW,kVar].
R_l, X_l	Resistance and reactance of branch l [Ω].
$\underline{VOL}_{i,\phi}$	Minimum squared voltage magnitude at node i in MG ϕ [kV^2].
$\overline{VOL}_{i,\phi}$	Maximum squared voltage magnitude at node i in MG ϕ [kV^2].
$P^F_{l,\phi}, Q^F_{l,\phi}$	Real/reactive power capacity of branch l in MG ϕ [kW,kVar].
$P^{UP}_{\psi}, Q^{UP}_{\psi}$	Real/reactive power limitation from upstream system ψ [kW,kVar].
$\underline{P}^{DG}_{g,\phi}, \overline{P}^{DG}_{g,\phi}$	Minimum/maximum real power capacity of DG unit g in MG ϕ [kW].
$\underline{Q}^{DG}_{g,\phi}, \overline{Q}^{DG}_{g,\phi}$	Minimum/maximum reactive power capacity of DG unit g in MG ϕ [kVar].
$\alpha^+_{g,\phi}, \alpha^-_{g,\phi}$	Ramp-up/ramp-down rate of DG unit g in MG ϕ [kW].
$\beta^+_{g,\phi}, \beta^-_{g,\phi}$	Start-up/shut-down limit of DG unit g in MG ϕ [kW].
$\gamma^+_{g,\phi}, \gamma^-_{g,\phi}$	Minimum up-time/down-time of DG unit g in MG g [h].
$\eta^{es-}_{e,\phi}, \eta^{es+}_{e,\phi}$	Charging/discharging efficiency of ESS unit e in MG ϕ.
$\underline{SOC}_{e,\phi}$	Minimum state of charge (SOC) of ESS unit e in MG ϕ [kWh].
$\overline{SOC}_{e,\phi}$	Maximum SOC of ESS unit e in MG ϕ [kWh].
$P^{ES-}_{e,\phi}$	Charging capacity of ESS unit e in MG ϕ

[kW].

$P^{ES+}_{e,\phi}$ Discharging capacity of ESS unit e in MG ϕ [kW].

$\underline{Q}^{ES}_{e,\phi}, \overline{Q}^{ES}_{e,\phi}$ Minimum/maximum reactive power output of ESS unit e in MG ϕ [kVar].

$P^{PV}_{\phi,t}$ Maximum solar energy that can be used in MG ϕ at time t [kW].

$K^{tr}_{m,n}$ Travel time for MWTs from TS node m to node n [h].

Cap_m Maximum number of MWT units that can be positioned at TS node m.

$\lambda_{m,\phi}$ Binary parameter equal to 1 if MG ϕ is located at TS node m.

P^{WT}_{w} Rated power of MWT unit w [kW].

$P^{W}_{\phi,t}$ Maximum wind energy that can be used in MG ϕ at time t [kW].

η^{th} Thermal discharge efficiency of ETS units.

η^{ets} Electric-thermal energy conversion efficiency of ETS units.

$\underline{\Pi}, \overline{\Pi}$ Minimum/Maximum thermal energy level of ETS units [kWh].

P^{ET} Limitation of electric input for electric heating element of ETS units [kW].

C. Decision Variables

$p^{u}_{\psi,\phi,t}, q^{u}_{\psi,\phi,t}$ Real/reactive power from the upstream system ψ to MG ϕ at time t [kW,kVar].

$p^{dg}_{g,\phi,t}, q^{dg}_{g,\phi,t}$ Real/reactive power output of DG unit g in MG ϕ at time t [kW,kVar].

$H^{ets}_{i,\phi,t}$ ETS effective thermal energy self-discharge at node i in MG ϕ at time t [kW].

$p^{es}_{e,\phi,t}, q^{es}_{e,\phi,t}$ Net real/reactive power from ESS e in MG ϕ at time t [kW,kVar].

$p^{f}_{l,\phi,t}, q^{f}_{l,\phi,t}$ Real/reactive power flow of branch l in MG ϕ at time t [kW,kVar].

$p^{pv}_{v,\phi,t}$ Power output of PV v in MG ϕ at time t [kW].

$p^{wt}_{w,\phi,t}$ Power output of MWT unit w in MG ϕ at time t [kW].

$p^{ete}_{i,\phi,t}, p^{eth}_{i,\phi,t}$ Electric input/thermal output for electric heating element of ETS units at node i in MG ϕ at time t [kW].

$\pi_{i,\phi,t}$ Thermal energy level of ETS unit at node i in MG ϕ at time t [kWh].

$\nu^{s}_{i,\phi,t}$ Squared voltage magnitude at node i in MG ϕ at time t [kV^2].

$p^{es-}_{e,\phi,t}, p^{es+}_{e,\phi,t}$ Charging/discharging power of ESS unit e in MG ϕ at time t [kW].

$x^{dg}_{g,\phi,t}$ Binary variable equal to 1 if DG unit g is online in MG ϕ at time t, 0 otherwise.

$y_{g,\phi,t}$ Binary variable equal to 1 if DG unit g starts up in MG ϕ at time t, 0 otherwise.

$z_{g,\phi,t}$ Binary variable equal to 1 if DG unit g shuts up in MG ϕ at time t, 0 otherwise.

$x^{es}_{e,\phi,t}$ Binary variable equal to 1 if ESS unit e is online in MG ϕ at time t, 0 otherwise.

$x^{es-}_{e,\phi,t}$ Binary variable equal to 1 if ESS unit e is charging in MG ϕ at time t, 0 otherwise.

$x^{es+}_{e,\phi,t}$ Binary variable equal to 1 if ESS unit e is discharging in MG ϕ at time t, 0 otherwise.

$x^{pv}_{v,\phi,t}$ Binary variable equal to 1 if PV unit v is online in MG ϕ at time t, 0 otherwise.

$x^{wt}_{w,\phi,t}$ Binary variable equal to 1 if MWT unit w is connected to MG ϕ at time t, 0 otherwise.

$u_{w,m,t}$ Binary variable equal to 1 if MWT unit w is located at TS node m at time t, 0 otherwise.

I. Introduction

Recently, the increasing penetration of renewable energy resources and improvements in the energy storage technologies have brought about more complexity to microgrid (MG) architectures, while enhance the effectiveness of energy management systems (EMSs) in lowering the system operating costs and increasing the efficiency measures. The utilization of renewable energy resources (e.g., wind and solar) within an EMS optimization of the MGs is widely discussed in [1]–[4]. Study [5] proposes an ultra-capacitor hybrid energy storage system (ESS) that can achieve a high-efficiency operation of the MGs. Beside the strategies mentioned above, electric thermal storage (ETS) and mobile wind turbine (MWT) units can also help efficiency enhancement in the MG operation.

By allowing for management of charging electric power and heat separately, an ETS unit can store thermal energy converted from electric energy during off-peak hours and discharge it for heating during peak hours [6]. A physics-based load model of ETS units is presented in [7]. The study in [8] discusses and analyzes the benefits and limitations of applying ETS supplied by wind-generated electricity to address issues of integrating intermittent renewables and electric space heating. A two-stage stochastic programming model for provision of flexible demand response based on ETS is presented in [9] to minimize the daily cost of electricity and gas import/export. The study in [10] proposes a price-based optimal control model for the combined demand response potential of the direct electric space heating and partial thermal storage, highlighting the benefits of demand response to aggregators. A mathematical model for an ETS is presented and integrated into a decoupled Unit Commitment and Optimal Power Flow-based EMS model in MG [11], where the benefits of integrating ETS are measured in terms of reducing operating costs, and load curtailment in the isolated MG.

Compared to stationary energy resources, such as diesel generators (DGs), solar panels, wind turbines, and ESSs, mobile power sources (MPSs) have promising potential for spatio-temporal flexibility exchange in MGs and have gained increasing attention for enhancing the efficiency of the MG operation and the resilience of power grids. The study in [12] proposes a day-ahead EMS model integrating MPSs to maximize the day-ahead profit and regulate the voltage level in power distribution systems. The study in [13] has proposed a two-stage restoration scheme with MPS utilization through a mixed-integer linear programming (MILP) model. A rolling

integrated service restoration strategy for scheduling and routing MPSs is introduced in [14], capturing the uncertainty in the status of the roads and electric branches. The study in [15] presents a restoration framework with joint probabilistic constraints to boost system resilience considering the application of MPSs. However, MPSs investigated in the literature [12]–[15] consume traditional energy to supply power, which have higher operating costs and harmful emissions. MWTs are transportable small-scale wind turbines that can unlock many applications in commercial, residential, government, military, and humanitarian markets [16]. The MWT is purposely designed to extract as much energy as possible from wind and keep parasitic losses to a minimum during the delivery process. Beyond low-cost power, the machine will be invaluable for EMS, in particular in rural areas, and other mobile operations that are constrained by the limitations of the power grid and/or availability of fuels.

The existing literature on EMS has not incorporated joint utilization of MWT and ETS into the MG energy portfolio. MWT offers a spatio-temporal flexibility to generating capacity, while ETS shifts demand profiles to make the most out of the renewable energy generation. This paper presents a new EMS model for all kinds of energy resources that operators could opt to include within their MG: solar, wind, battery storage, thermal storage, mobile energy sources, and traditional generation. To demonstrate the benefits of this unified model, an MILP optimization problem is constructed to evaluate the performance of EMS for joint operation of MWT and ETS units. The model performance is verified on an integrated test system: a Sioux Falls transportation network and four IEEE 33-node distribution systems.

The rest of this paper is organized as follows: Section II introduces the proposed EMS optimization model, Section III discusses numerical results, and Section IV summarizes the research findings.

II. Problem Formulation

In this section, we propose a new EMS optimization model that explicitly accounts for joint operation of MWT and ETS in isolated MGs. The proposed model is formulated as an MILP optimization problem with the following objective function:

$$\min \sum_{\phi\in\mathbf{\Phi}}\sum_{t\in\mathbf{T}}\Big[\sum_{\psi\in\mathbf{\Psi}} c^{up}_{\psi,t}p^{u}_{\psi,\phi,t}+\sum_{g\in\mathbf{G}}(a_g p^{dg}_{g,\phi,t}+b_g x^{dg}_{g,\phi,t} + c^{su}_g y_{g,\phi,t}+c^{sd}_g z_{g,\phi,t})+\sum_{i\in\mathbf{B}} c^{ets}\mu_{\phi,t}H^{ets}_{i,\phi,t}\Big] \quad (1)$$

The objective function (1) aims to minimize the total operating cost through effective management of MWT and ETS in MGs. The first term represents the cost of power obtained from upstream systems. The second term indicates the operating costs of DGs, including generation, no-load, start-up, and shut-down costs. The third term reflects the operating cost of ETS [11]. The proposed optimization model has a mixed-integer linear feasible set defined by the operation constraints (on MGs, DGs, ESSs, renewable energy, and ETS) described in the following subsections II-A to II-E.

A. Microgrids Operation Constraints

Constraints (2a) and (2b) describe the real and reactive power balance conditions at each node in MGs. The energy resources include: power from the upstream system, DG power generation, ESS net output, solar energy from PV, and wind power from MWT. The term $\delta_{\phi,t}P^{d}_{i,\phi,t}$ in constraint (2a) indicates the required demand for electric heating. To ease the notations, we define the index set $\mathbb{V}=\{(i,j,l,\phi,t): i,j\in\mathbf{B}, l\in\mathbf{L}, \phi\in\mathbf{\Phi}, t\in\mathbf{T}\}$. Constraint (2c) represents the power flow equations within MGs with radial architecture [17]. Constraints (2d)-(2h) state the limits for the squared voltage magnitudes, real/reactive power flow, and real/reactive power from upstream systems, respectively.

$$\begin{aligned}&\sum_{l(j,i)\in\mathbf{L}} p^{f}_{l,\phi,t}+\sum_{\psi\in\mathbf{\Psi}_i} p^{u}_{\psi,\phi,t}+\sum_{g\in\mathbf{G}_i} p^{dg}_{g,\phi,t}+\sum_{e\in\mathbf{E}_i} p^{es}_{e,\phi,t}\\ &+\sum_{v\in\mathbf{V}_i} p^{pv}_{v,\phi,t}+\sum_{w\in\mathbf{W}_i} p^{wt}_{w,\phi,t}\\ =&\sum_{l(i,j)\in\mathbf{L}} p^{f}_{l,\phi,t}+\Big((1-\delta_{\phi,i})+(1-\mu_{\phi,i})\delta_{\phi,i}\Big)P^{d}_{i,\phi,t}\\ &+\mu_{\phi,i}p^{ete}_{i,\phi,t} \qquad i\in\mathbf{B},\phi\in\mathbf{\Phi},t\in\mathbf{T} \quad (2a)\\ &\sum_{l(j,i)\in\mathbf{L}} q^{f}_{l,\phi,t}+\sum_{\psi\in\mathbf{\Psi}_i} q^{u}_{\psi,\phi,t}+\sum_{g\in\mathbf{G}_i} q^{dg}_{g,\phi,t}+\sum_{e\in\mathbf{E}_i} q^{es}_{e,\phi,t}\\ =&\sum_{l(i,j)\in\mathbf{L}} q^{f}_{l,\phi,t}+Q^{d}_{i,\phi,t} \qquad i\in\mathbf{B},\phi\in\mathbf{\Phi},t\in\mathbf{T} \quad (2b)\\ &\nu^{s}_{i,\phi,t}-\nu^{s}_{j,\phi,t}=2(R_l p^{f}_{l,\phi,t}+X_l q^{f}_{l,\phi,t}) \quad (i,j,l,\phi,t)\in\mathbb{V} \quad (2c)\\ &\underline{VOL}^{S}_{i,\phi}\le\nu^{s}_{i,\phi,t}\le\overline{VOL}^{S}_{i,\phi} \qquad i\in\mathbf{B},\phi\in\mathbf{\Phi},t\in\mathbf{T} \quad (2d)\\ &-P^{F}_{l,\phi}\le p^{f}_{l,\phi,t}\le P^{F}_{l,\phi} \qquad l\in\mathbf{L},\phi\in\mathbf{\Phi},t\in\mathbf{T} \quad (2e)\\ &-Q^{F}_{l,\phi}\le q^{f}_{l,\phi,t}\le Q^{F}_{l,\phi} \qquad l\in\mathbf{L},\phi\in\mathbf{\Phi},t\in\mathbf{T} \quad (2f)\\ &0\le p^{u}_{\psi,\phi,t}\le P^{UP}_{\psi} \qquad \psi\in\mathbf{\Psi},\phi\in\mathbf{\Phi},t\in\mathbf{T} \quad (2g)\\ &0\le q^{u}_{\psi,\phi,t}\le Q^{UP}_{\psi} \qquad \psi\in\mathbf{\Psi},\phi\in\mathbf{\Phi},t\in\mathbf{T} \quad (2h)\end{aligned}$$

B. Diesel Generators Operation Constraints

In this subsection, we define the index sets $\mathbb{G}=\{(g,\phi,t): g\in\mathbf{G},\phi\in\mathbf{\Phi},t\in\mathbf{T}\}$ and $\mathbb{G}'=\{(g,\phi,t): g\in\mathbf{G},\phi\in\mathbf{\Phi},t\in\mathbf{T}\setminus\{1\}\}$. Constraint (3a) denotes the relationship between the DG's start-up and shut-down statuses based on its dispatch schedules. Constraint (3b) guarantees that each DG unit cannot start up and shut down at the same time. Each DG unit has a ramp rate, start-up and shut-down limits to restrict the changes in power output over time, which are modelled by constraints (3c) and (3d). Constraints (3e) and (3f) represent the minimum up-time and down-time constraints for DG unit g in MG ϕ. Constraints (3g) and (3h) specify the boundaries for real and reactive power output of DG unit g in MG ϕ, while the binary variable $x^{dg}_{g,\phi,t}=0$ assures that the real and reactive power outputs are equal to 0.

$$\begin{aligned}&y_{g,\phi,t}-z_{g,\phi,t}=x^{dg}_{g,\phi,t}-x^{dg}_{g,\phi,t-1} \qquad (g,\phi,t)\in\mathbb{G}' \quad (3a)\\ &y_{g,\phi,t}+z_{g,\phi,t}\le 1 \qquad (g,\phi,t)\in\mathbb{G} \quad (3b)\\ &p^{dg}_{g,\phi,t}-p^{dg}_{g,\phi,t-1}\le\alpha^{+}_{g,\phi}(1-y_{g,\phi,t})+\beta^{+}_{g,\phi}y_{g,\phi,t} \qquad (g,\phi,t)\in\mathbb{G}' \quad (3c)\end{aligned}$$

$$p^{dg}_{g,\phi,t-1} - p^{dg}_{g,\phi,t} \le \alpha^{-}_{g,\phi}(1 - z_{g,\phi,t}) + \beta^{-}_{g,\phi} z_{g,\phi,t} \quad (g,\phi,t) \in \mathbb{G}' \quad (3d)$$

$$y_{g,t} \le x^{dg}_{g,\tau} \quad (g,\phi,t) \in \mathbb{G}, \tau \in [t, min(\gamma^{+}_{g,\phi} + t, |\mathbf{T}|)] \quad (3e)$$

$$z_{g,t} \le 1 - x^{dg}_{g,\tau} \quad (g,\phi,t) \in \mathbb{G}, \tau \in [t, min(\gamma^{-}_{g,\phi} + t, |\mathbf{T}|)] \quad (3f)$$

$$\underline{P}^{DG}_{g,\phi} x^{dg}_{g,\phi,t} \le p^{dg}_{g,\phi,t} \le \overline{P}^{DG}_{g,\phi} x^{dg}_{g,\phi,t} \quad (g,\phi,t) \in \mathbb{G} \quad (3g)$$

$$\underline{Q}^{DG}_{g,\phi} x^{dg}_{g,\phi,t} \le q^{dg}_{g,\phi,t} \le \overline{Q}^{DG}_{g,\phi} x^{dg}_{g,\phi,t} \quad (g,\phi,t) \in \mathbb{G} \quad (3h)$$

C. Energy Storage System Operation Constraints

To ease the notations, we define the index sets $\mathbb{E} = \{(g,\phi,t) : e \in \mathbf{E}, \phi \in \mathbf{\Phi}, t \in \mathbf{T}\}$ and $\mathbb{E}' = \{(g,\phi,t) : e \in \mathbf{E}, \phi \in \mathbf{\Phi}, t \in \mathbf{T} \setminus \{1\}\}$. The variations in the state of charge (SOC) of ESSs over time is determined by their charging and discharging behaviors, as denoted in constraint (4a). Constraint (4b) restricts the range of SOC of ESSs. Constraint (4c) indicates that charging and discharging of ESSs are mutually exclusive. Constraints (4d) and (4e) impose the limits for charging and discharging power of ESS units, respectively. The net real power output of ESSs is bounded by constraint (4f). Constraint (4g) specifies the boundary for reactive power output of the ESS units.

$$SOC_{e,\phi,t} - SOC_{e,\phi,t-1} = \eta^{es-}_{e,\phi} p^{es-}_{e,\phi,t-1} - p^{es+}_{e,\phi,t-1}/\eta^{es+}_{e,\phi} \quad (e,\phi,t) \in \mathbb{E}' \quad (4a)$$

$$\underline{SOC}_{e,\phi} \le SOC_{e,\phi,t} \le \overline{SOC}_{e,\phi} \quad (e,\phi,t) \in \mathbb{E} \quad (4b)$$

$$x^{es+}_{e,\phi,t} + x^{es-}_{e,\phi,t} \le x^{es}_{e,\phi,t} \quad (e,\phi,t) \in \mathbb{E} \quad (4c)$$

$$0 \le p^{es-}_{e,\phi,t} \le P^{ES-}_{e,\phi,t} \quad (e,\phi,t) \in \mathbb{E} \quad (4d)$$

$$0 \le p^{es+}_{e,\phi,t} \le P^{ES+}_{e,\phi,t} \quad (e,\phi,t) \in \mathbb{E} \quad (4e)$$

$$p^{es}_{e,\phi,t} = p^{es+}_{e,\phi,t} - p^{es-}_{e,\phi,t} \quad (e,\phi,t) \in \mathbb{E} \quad (4f)$$

$$x^{es}_{e,\phi,t}\underline{Q}^{es}_{e,\phi,t} \le q^{es}_{e,\phi,t} \le x^{es}_{e,\phi,t}\overline{Q}^{es}_{e,\phi,t} \quad (e,\phi,t) \in \mathbb{E} \quad (4g)$$

D. Renewable Energy Operation Constraints

In this study, there are two sources of renewable energy within each MG — PV installed ex-ante and MWT assigned by system operators. Constraint (5a) denotes the range of power output for PV unit v in MG ϕ at time period t. The operation of MWTs is modelled by constraints (5b) – (5h). Each MWT unit w can stay in at most one TS node at any time period, which is enforced by constraint (5b). The routing of MWTs is defined by constraint (5c). Constraint (5d) specifies the initial location of MWTs which are all positioned at the depot. Constraint (5e) ensures that the total number of MWTs located at TS node m at any time period does not exceed the maximum number of vehicles that node m can host. Constraint (5f) restricts that MWT m can be connected to MG ϕ only if it reaches the TS node m, at the location of MG ϕ. Constraint (5g) indicates the power output of MWTs over all time periods. The total power output of MWTs cannot exceed the maximum wind energy that can be used in MG ϕ at time t, which is denoted by constraint (5h).

$$0 \le p^{pv}_{v,\phi,t} \le P^{PV}_{\phi,t} x^{pv}_{v,\phi,t} \quad v \in \mathbf{V}, \phi \in \mathbf{\Phi}, t \in \mathbf{T} \quad (5a)$$

$$\sum_{m \in \mathbf{M}} u_{w,m,t} \le 1 \quad w \in \mathbf{W}, m \in \mathbf{N}, t \in \mathbf{T} \quad (5b)$$

$$u_{w,n,t+\tau} \le 1 - u_{w,m,t} \quad w \in \mathbf{W}, m,n \in \mathbf{N}, \tau \le K^{tr}_{m,n}, t \le |\mathbf{T}| - \tau \quad (5c)$$

$$u_{w,m,1} = 1 \quad w \in \mathbf{W}, m \in \mathbf{N^d} \quad (5d)$$

$$\sum_{w \in \mathbf{W}} u_{w,m,t} \le Cap_m \quad m \in \mathbf{N}, t \in \mathbf{T} \quad (5e)$$

$$u_{w,m,t} \ge \lambda_{m,\phi} x^{wt}_{w,\phi,t} \quad w \in \mathbf{W}, m \in \mathbf{N}\phi \in \mathbf{\Phi}, t \in \mathbf{T} \quad (5f)$$

$$p^{wt}_{w,\phi,t} = P^{WT}_{w} x^{wt}_{w,\phi,t} \quad w \in \mathbf{W}, \phi \in \mathbf{\Phi}, t \in \mathbf{T} \quad (5g)$$

$$\sum_{w \in \mathbf{W}} p^{wt}_{w,\phi,t} \le P^{W}_{\phi,t} \quad \phi \in \mathbf{\Phi}, t \in \mathbf{T} \quad (5h)$$

E. Electric Thermal Storage Operation Constraints

Constraints (6a) – (6e) represent ETS operation within MGs over all time periods. The change in ETS thermal energy level is denoted by constraint (6a). Constraint (6b) indicates the characteristics of the effective thermal energy self-discharge of ETS [11]. Constraint (6c) represents the relationship between electric input and thermal output for electric heating element of ETS. Constraints (6d) and (6e) state the limits for ETS thermal energy level and electric input of ETS, respectively.

$$\pi_{i,\phi,t} - \pi_{i,\phi,t-1} = p^{eth}_{i,\phi,t-1} - \delta_{\phi,t-1} P^{d}_{i,\phi,t-1} - H^{ets}_{i,\phi,t-1} \quad i \in \mathbf{B}, \phi \in \mathbf{\Phi}, t \in \mathbf{T} \setminus \{1\} \quad (6a)$$

$$H_{i,\phi,t} \ge (1 - \eta^{th})\pi_{i,\phi,t} - \delta_{\phi,t} P^{d}_{i,\phi,t} \quad i \in \mathbf{B}, \phi \in \mathbf{\Phi}, t \in \mathbf{T} \quad (6b)$$

$$p^{eth}_{i,\phi,t} = \eta^{ets} p^{ete}_{i,\phi,t} \quad i \in \mathbf{B}, \phi \in \mathbf{\Phi}, t \in \mathbf{T} \quad (6c)$$

$$\underline{\Pi} \le \pi_{i,\phi,t} \le \overline{\Pi} \quad i \in \mathbf{B}, \phi \in \mathbf{\Phi}, t \in \mathbf{T} \quad (6d)$$

$$0 \le p^{ete}_{i,\phi,t} \le P^{ET} \quad i \in \mathbf{B}, \phi \in \mathbf{\Phi}, t \in \mathbf{T} \quad (6e)$$

III. Numerical Results

A. Test System Description

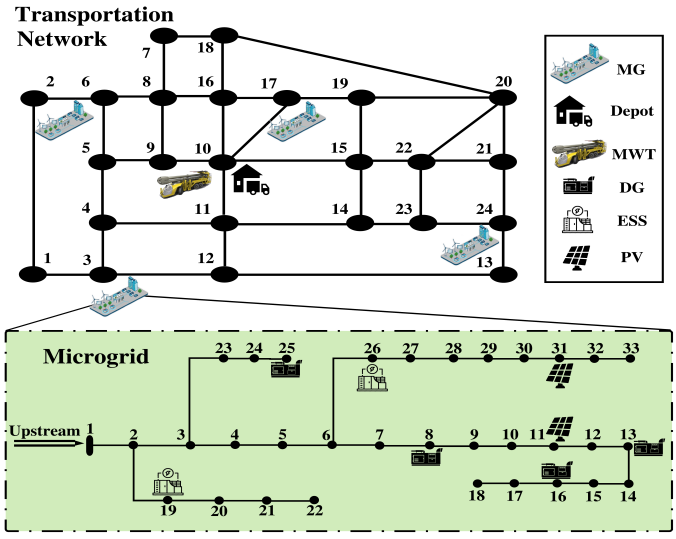

Fig. 1. An integrated test system with a Sioux Falls transportation network and four microgrids.

In this section, the effectiveness of the proposed EMS model is verified by application to a test case that integrates a transportation system and multiple isolated microgrids; that is, a Sioux Falls transportation network [18] and four IEEE 33-node distribution systems [19] (see Figure 1). To investigate

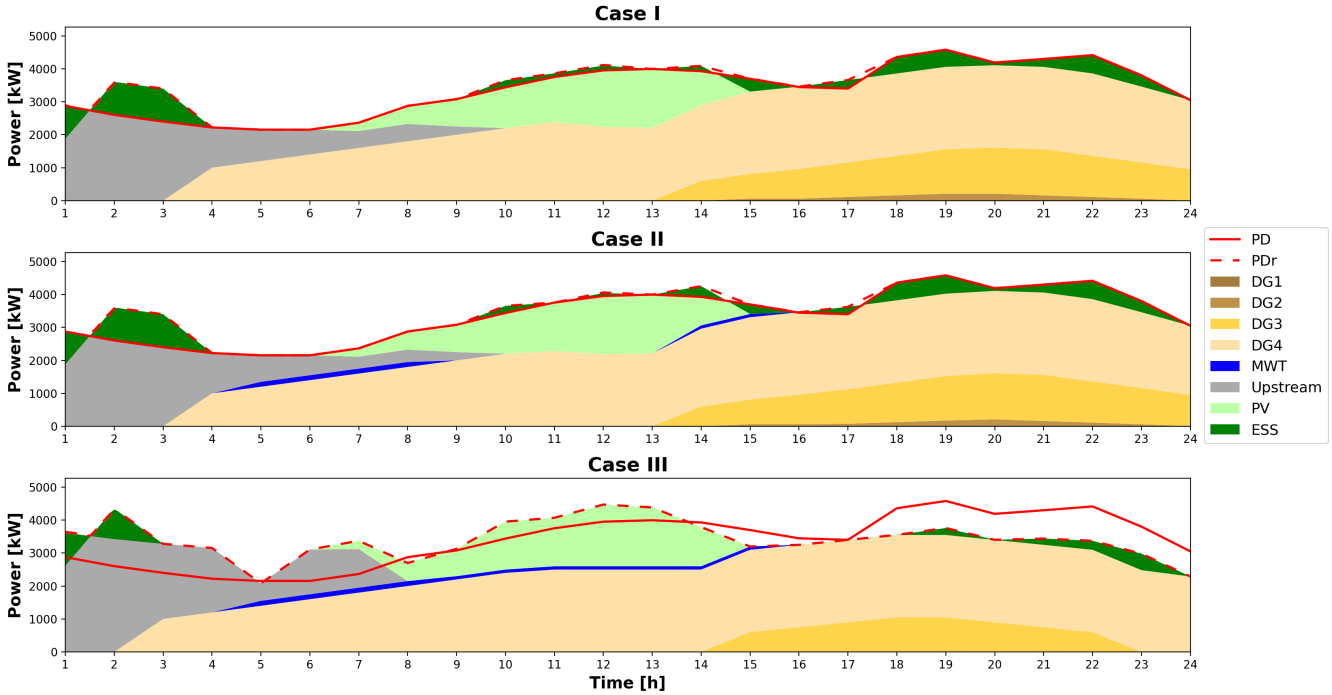

Fig. 2. Dispatch for all three cases in the **Microgrid 3**

the impact of joint operation of MWT and ETS units on the energy management of the MGs, we here study three different cases on this test system: ***Case I*** includes neither MWT nor ETS units; ***Case II*** allows the EMS to command MWT without the presence of ETS, and ***Case III*** involves both MWT and ETS participation within the EMS optimization. Eight MWTs are considered in the test system, each with the rated power set to be 50 kW [20]. The detailed information on ETS units can be found in [21]. The operating costs of DGs, including generation, no-load, start-up, and shut-down costs, are the same in each MG, which are presented in Table I. All simulations have been conducted on a PC with an Intel Xeon E5-2620 processor and 16 GB of memory using AMPL with the optimization solver Gurobi 9.0.2.

TABLE I
THE OPERATING COSTS OF DGS

Unit	a_g	b_g	c_g^{su}	c_g^{sd}
DG1	0.2881	7.5	15	5.3
DG2	0.2876	0	7.35	1.44
DG3	0.2571	25.5	4.5	8.3
DG4	0.224	45.5	9.5	15.3

B. Analysis and Discussions

Table II presents a summary of the results in all studied cases. Based on the results presented in Table II, one can observe that (i) the operating cost of the integrated test system is reduced from ***Case I*** to ***Case III***, which highlights that the application of MWT and ETS can lower the operating cost of the energy systems, (ii) DG1 — the most expensive generator — is dispatched less during the total time span in all cases, while the dispatch percentage of the second-most expensive generator DG2 decreases sharply from ***Case I*** to ***Case III***, (iii) The dispatch percentage of ESS is the least in ***Case III***, where the ETS is utilized.

TABLE II
SUMMARY OF THE RESULTS IN ALL STUDIED CASES

Case	Operating Cost	Dispatch Percentage (%)		
	[$]	DG1	DG2	ESS
I	79477.6	11.6	50	35.9
II	77540.6	10.3	39.7	35.9
III	76513.5	0	0	13

Figure 2 presents stacked-area plots of the optimal dispatch obtained for all studied cases in **Microgrid 3**. The red solid line represents the forecasted demand (PD), while the red dashed-line indicates the total real-time demand including forecasted demand required by costumers, ESS charging, and ETS electric input ($PDr = PD + P^{ES-} + P^{ETS}$). Compared to ***Case I*** and ***Case II***, the real-time demand profile is significantly different with that of the forecasted demand in ***Case III***. During the time periods $t1$–$t6$, where the purchase price of power from upstream systems is low, and the time periods $t7$–$t15$, where the solar energy is sufficient and MWTs are connected, ETS consumes more electric power to store extra thermal energy. When the power purchase price from the upstream system is high and the renewable energy has decreased ($t16$–$t24$), ETS discharges the heat, leading to less energy required for electric heating.

The optimal routing and scheduling of MWTs in the test system for ***Case II*** and ***Case III*** is presented in Figure 3. The assignments of MWTs 1-3, MWTs 5-6, MWT 8 are the same in both cases. MWTs 4 and 7 supply wind energy to **Microgrid 3** during less time intervals in ***Case II*** than in ***Case III*** ($t14$–$t15$ in ***Case II*** vs. $t9$–$t15$ in ***Case III***).

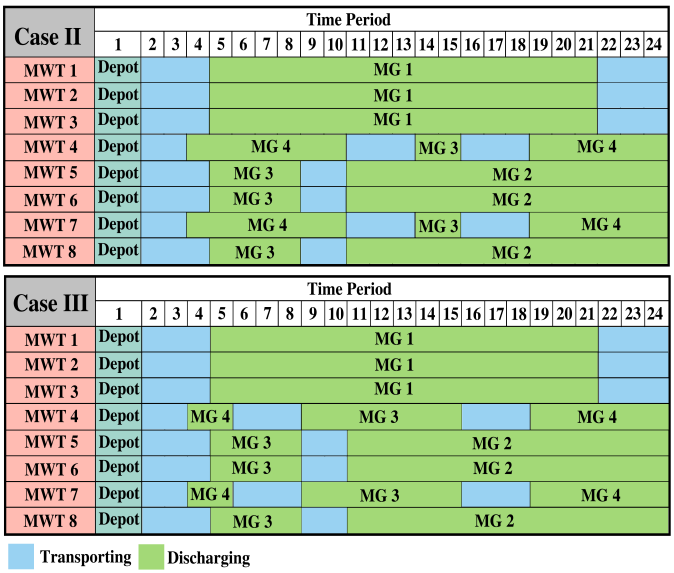

Fig. 3. The optimal routing and scheduling of MWT units in the integrated test system.

Verifying the proposed EMS model by numerical case studies, we can make several observations:

- Including MWT and ETS in an EMS model can significantly decrease operating cost of MGs by reducing power drawn from upstream systems and power produced from more expensive DGs.
- ETS can shift the demand profile by charging during off-peak hours or hours with sufficient renewable energy, and discharging during peak hours or hours with insufficient renewable energy.
- The routing and scheduling of MWTs will vary with the participation of ETS, as optimally decided by the proposed EMS model.

IV. Conclusion

In this paper, we developed an EMS model for joint operation of MWT and ETS in isolated MGs. The proposed model is formulated as an MILP optimization problem and implemented on an integrated test system with a Sioux Falls transportation network and four IEEE 33-node distribution systems. Extensive numerical results highlight that the application of MWT and ETS can significantly reduce the operating cost of MGs. The primary driver for this cost reduction is the generating flexibility and energy storing capabilities offered by MWT and ETS. These technologies, when managed by an effective EMS, can shift the load profile of a MG and prevent costs associated with peak demand. Future research could employ stochastic or robust optimization to discuss the impact of uncertain wind energy distribution on the routing and scheduling of MWT.

V. Acknowledgment

This work was supported in part by the U.S. National Science Foundation (NSF) under Grants ICER-2022505 and ECCS-2114100.

References

[1] D. E. Olivares, C. A. Cañizares, and M. Kazerani, "A centralized energy management system for isolated microgrids," *IEEE Transactions on Smart Grid*, vol. 5, no. 4, pp. 1864–1875, 2014.

[2] B. Zhao, X. Wang, D. Lin, M. M. Calvin, J. C. Morgan, R. Qin, and C. Wang, "Energy management of multiple microgrids based on a system of systems architecture," *IEEE Transactions on Power Systems*, vol. 33, no. 6, pp. 6410–6421, 2018.

[3] J. Han, C. Choi, W. Park, I. Lee, and S. Kim, "Smart home energy management system including renewable energy based on zigbee and plc," *IEEE Transactions on Consumer Electronics*, vol. 60, no. 2, pp. 198–202, 2014.

[4] W. Jiang, K. Yang, J. Yang, R. Mao, N. Xue, and Z. Zhuo, "A multiagent-based hierarchical energy management strategy for maximization of renewable energy consumption in interconnected multi-microgrids," *IEEE Access*, vol. 7, pp. 169931–169945, 2019.

[5] J. Shen and A. Khaligh, "A supervisory energy management control strategy in a battery/ultracapacitor hybrid energy storage system," *IEEE Transactions on Transportation Electrification*, vol. 1, no. 3, pp. 223–231, 2015.

[6] W. R. Coleman and C. M. Grastataro, "American electric power system electric thermal storage program: an evaluation of performance within the home," *IEEE Transactions on Power Apparatus and Systems*, vol. PAS-100, no. 12, pp. 4741–4749, 1981.

[7] A. Molina, A. Gabaldon, C. Alvarez, J. Fuentes, and E. Gómez, "A physically based load model of residential electric thermal storage: Application to lm programs," *International Journal of Power and Energy Systems*, vol. 24, no. 1, pp. 24–31, 2004.

[8] L. Hughes, "Meeting residential space heating demand with wind-generated electricity," *Renewable Energy*, vol. 35, no. 8, pp. 1765–1772, 2010.

[9] N. Good, E. Karangelos, A. Navarro-Espinosa, and P. Mancarella, "Optimization under uncertainty of thermal storage-based flexible demand response with quantification of residential users' discomfort," *IEEE Transactions on Smart Grid*, vol. 6, no. 5, pp. 2333–2342, 2015.

[10] M. Ali, J. Jokisalo, K. Siren, and M. Lehtonen, "Combining the demand response of direct electric space heating and partial thermal storage using LP optimization," *Electric Power Systems Research*, vol. 106, pp. 160–167, 2014.

[11] P. S. Sauter, B. V. Solanki, C. A. Cañizares, K. Bhattacharya, and S. Hohmann, "Electric thermal storage system impact on northern communities' microgrids," *IEEE Transactions on Smart Grid*, vol. 10, no. 1, pp. 852–863, 2019.

[12] H. H. Abdeltawab and Y. A. I. Mohamed, "Mobile energy storage scheduling and operation in active distribution systems," *IEEE Transactions on Industrial Electronics*, vol. 64, no. 9, pp. 6828–6840, 2017.

[13] Z. Yang, P. Dehghanian, and M. Nazemi, "Seismic-resilient electric power distribution systems: Harnessing the mobility of power sources," *IEEE Transactions on Industry Applications*, vol. 56, no. 3, pp. 2304–2313, 2020.

[14] S. Yao, P. Wang, X. Liu, H. Zhang, and T. Zhao, "Rolling optimization of mobile energy storage fleets for resilient service restoration," *IEEE Transactions on Smart Grid*, vol. 11, no. 2, pp. 1030–1043, 2020.

[15] M. Nazemi, P. Dehghanian, X. Lu, and C. Chen, "Uncertainty-aware deployment of mobile energy storage systems for distribution grid resilience," *IEEE Transactions on Smart Grid*, vol. 12, no. 4, pp. 3200–3214, 2021.

[16] D. Anokhin, P. Dehghanian, M. A. Lejeune, and J. Su, "Mobility-as-a-service for resilience delivery in power distribution systems," *Production and Operations Management*, 2021.

[17] M. Baran and F. Wu, "Network reconfiguration in distribution systems for loss reduction and load balancing," *IEEE Transactions on Power Delivery*, vol. 4, no. 2, pp. 1401–1407, 1989.

[18] L. J. LeBlanc, E. K. Morlok, and W. P. Pierskalla, "An efficient approach to solving the road network equilibrium traffic assignment problem," *Transportation research*, vol. 9, no. 5, pp. 309–318, 1975.

[19] D. N. Trakas and N. D. Hatziargyriou, "Optimal distribution system operation for enhancing resilience against wildfires," *IEEE Transactions on Power Systems*, vol. 33, no. 2, pp. 2260–2271, 2018.

[20] "Portable Wind Turbine." [Online] Available: https://upriseenergy.com/50kw-portable-power-center.

[21] "STEFFES ETS Room Units." [Online] Available: https://www.steffes.com/electric-thermal-storage/room-units/.